

The mouse polydactylous mutation, *luxate (lx)*, causes anterior shift of the anteroposterior border in the developing hindlimb bud

YUKARI YADA^{1,2}, SHIGERU MAKINO², SADAO CHIGUSA-ISHIWA¹ and TOSHIHIKO SHIROISHI^{*,2}

¹Ochanomizu University, Tokyo and ²Mammalian Genetics Laboratory, National Institute of Genetics, Shizuoka, Japan

ABSTRACT Pattern formation along the anterior-posterior axis of the vertebrate limb is established upon activation of Sonic Hedgehog (SHH) in the zone of polarizing activity (ZPA). Since many mouse mutants with preaxial polydactyly show ectopic expression of *Shh* at the anterior margin of the limb buds, it has been thought to be a primary defect caused by these mutations. We show here that the mouse mutation *luxate (lx)* exhibits dose-dependent reduction in the size of the *Fgf8* expression domain in the ectoderm from the initial stage of limb development. This aberration was independent of *Fgf10* expression in the limb mesenchyme. *Shh* was induced in the mesenchyme underlying the posterior end of the *Fgf8* expression domain, indicating an anterior shift of *Shh* expression in *lx* hindlimb buds. Prior to the ectopic induction of *Shh*, the expression domains of genes downstream from *Shh*, namely *dHAND*, *Gli1*, *Ptc* and *Gre*, which are normally expressed in posterior mesenchyme of limb buds, expanded anteriorly on the *lx* hindlimb buds. Conversely, the expression domains of anterior mesenchymal markers such as *Gli3* and *Alx4* decreased in size. Thus, ectopic *Shh* is not a primary defect of the *lx* mutation. Rather, our results indicate that the *lx* mutation affects the positioning of the anteroposterior border in developing hindlimb buds.

KEY WORDS: *luxate*, limb development, *Shh*, *Fgf-8*, *d-HAND*

Introduction

Limb development is one of the classical model systems that have been used for studying vertebrate morphogenesis. Pattern formation of limbs requires coordinate signals along the anteroposterior (A-P) and the proximodistal (P-D) axes. The A-P axis is controlled by the zone of polarizing activity (ZPA), located at the posterior margin of the limb bud. Grafting of the ZPA to the anterior margin of chick limb bud results in a mirror-image duplication of the anterior digits (Saunders and Gasseling, 1968; Tickle *et al.*, 1975; Tickle, 1981). Sonic hedgehog (*Shh*) is expressed in the region corresponding to the ZPA and is thought to mediate ZPA activity (Riddle *et al.*, 1993).

Pattern formation and continued outgrowth along the P-D axis is controlled by the thickened epithelium located at the distal tip of limb buds, called the apical ectodermal ridge (AER) (Saunders, 1948). Previous studies suggested that several members of the *Fgf* family expressed in the AER control limb outgrowth (Niswander *et al.*, 1993; Crossley *et al.*, 1996). When limb outgrowth is initiated, *Fgf8* is activated in the intermediate mesoderm by unknown signal(s), and *Fgf8* induces *Fgf10* in the lateral plate mesoderm. The mesenchyme expressing *Fgf10* bulges from the trunk and

forms limb buds. *Fgf10* in the limb mesenchyme then induces the expression of *Fgf8* in the distal epithelium and subsequently in the AER (Ohuchi *et al.*, 1997).

Formation of the proper limb axis requires interaction between ZPA and AER signals. *Fgf4*, *Fgf9* and *Fgf17* are expressed in the posterior two-thirds of the AER, and their expression is maintained by *Shh*. In conditional mutants of *Fgf4*, *Fgf9* and *Fgf17*, expression of *Shh* and morphology of the resulting limbs are normal (Colvin *et al.*, 1999; Sun *et al.*, 2000). On the other hand, conditional disruption of *Fgf8* in the AER results in reduced limb size and a delay of *Shh* expression (Lewandoski *et al.*, 2000; Moon *et al.*, 2000). These data suggest that a positive feedback loop exists between *Shh* and the combined activities of two or more *Fgfs*, and that *Fgf8* alone has a distinct role in promoting cell proliferation and inducing *Shh* expression in normal limb development.

Gremlin (*Gre*) is a member of the DAN family of BMP antagonists and blocks BMP2, BMP4 and BMP7 signaling (Hsu *et al.*,

Abbreviations used in this paper: AER, apical ectodermal ridge; Fgf, fibroblast growth factor; lx, luxate; Shh, sonic hedgehog; ZPA, zone of polarizing activity.

*Address correspondence to: Dr. Toshihiko Shiroishi, Mammalian Genetics Laboratory, National Institute of Genetics, Yata 1111, Mishima-shi, Shizuoka 411-8540, Japan. Fax: +81-55-981-6817. e-mail: tshirois@lab.nig.ac.jp

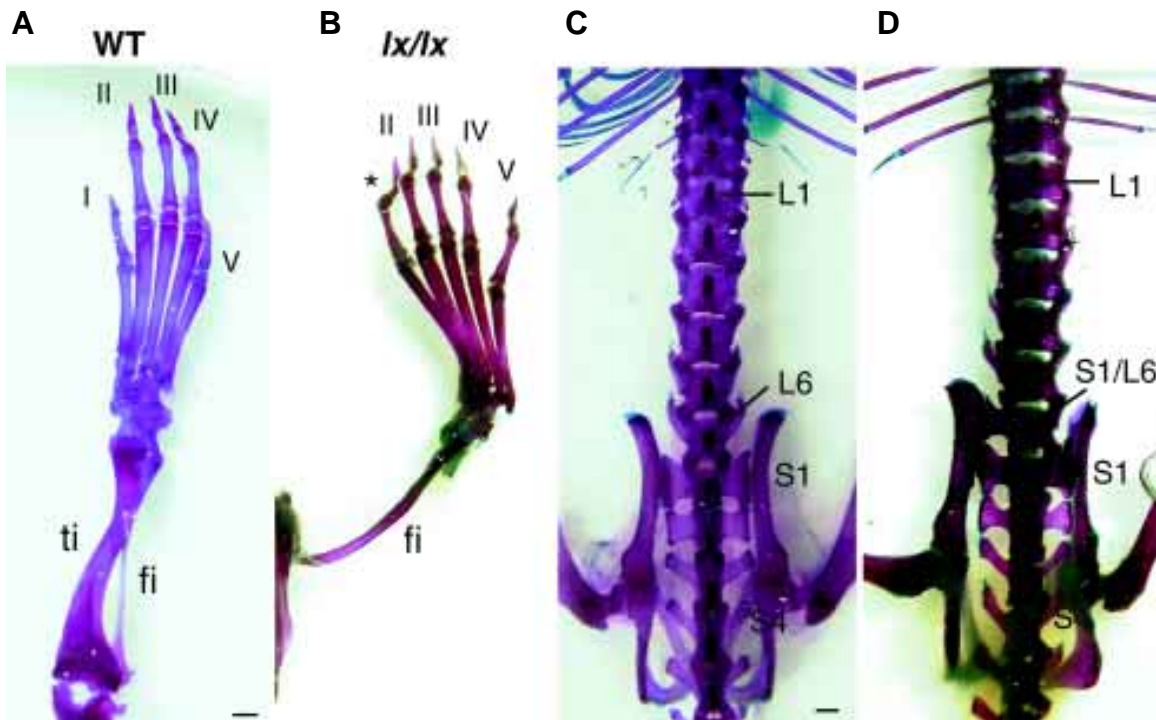


Fig. 1. Skeletal phenotype of the adult hindlimb region of wild-type and *lx* homozygotes. (A) Dorsal view of the wild-type hindlimb, illustrating normal morphology of the tibia (ti), fibula (fi) and digits (I through V). (B) The right hindlimb of the *lx* mutant shows hyperphalangy of the most anterior digit (asterisk) with absence of the tibia and malformation of the fibula. (C) Wild-type mouse with four sacral vertebrae (S1 through S4) following the sixth lumbar vertebrae (L6; the 26th vertebra). (D) The 26th vertebra of *lx* mutant mice is a lumbar-sacral transitional form (S1/L6), indicating anterior shift of the leg position. Scale bar, 1 mm.

1998). In developing limb buds, *Gre* maintains AER and *Fgf4* expression through inhibition of BMP signaling, while *Gre* is maintained by *Shh* (Capdevila et al., 1999; Merino et al., 1999; Zúñiga et al., 1999). Thus, *Gre* mediates the feedback loop between *Shh* and *Fgf4*.

Many genes are known to be involved in restricting *Shh* expression to the posterior side of limb buds. *Gli3* and *Alx4* are expressed in the anterior region of the mesenchyme, which is complementary to the *Shh* expression domain. These two genes are thought to repress *Shh* in normal limb development (Masuya et al., 1997; Qu et al., 1997). Disruption of *Gli3* and *Alx4* causes ectopic expression of *Shh* and polydactylous phenotypes in extra-toes-Jackson (*Xt'*) and Strong's luxoid (*Ist*) (Hui and Joyner, 1993; Masuya et al., 1997; Qu et al., 1998). *dHAND* is expressed in posterior mesenchyme and activates *Shh* expression. Overexpression of *dHAND* in the whole mouse limb bud causes ectopic induction of *Shh* and activation of *Shh* downstream genes, which consequently results in preaxial polydactyly (Charité et al., 2000).

Mutants with preaxial polydactyly compose a major form of limb abnormalities in mouse. Ectopic expression of *Shh* and *Fgf4* is a general phenomenon in mutants such as *Xt'*, *Ist*, Recombinant induced mutant 4 (*Rim4*), Hemimelic extra toe (*Hx*) and X-linked polydactyly (*Xpl*) (Masuya et al., 1995; Masuya et al., 1997). Although these genes likely have a function to repress *Shh* expression in normal limb development, mechanism of the suppression is poorly understood. Moreover, it remains open by what mechanism the expression domains of *Gli3* and *Alx4* are restricted to the anterior side in the limb mesenchyme.

luxate (*lx*) is a spontaneous limb mutant that has been mapped to the proximal region of Chromosome 5 (Lane, 1967). *lx* mutants show preaxial polydactyly, which is restricted to the hindlimbs. Homozygotes show polydactyly, oligodactyly, hemimelia with shortened tibias, and sacralization of the 26th vertebra (Carter, 1951). In addition to the skeletal anomalies, they have various kidney defects such as horseshoe kidney, polycystic kidney and hydronephrosis (Carter, 1953). *lx* mutants have been reported to exhibit ectopic *Shh* expression in the hindlimb buds (Masuya et al., 1997). To elucidate the defect responsible for the phenotype in *lx* mutants and to study the interaction between the *lx* gene and other key genes known to function in limb development, we examined the expression of these key genes in early stage *lx* mutant embryos. In this study, we show that *lx* mutants exhibit anterior-restricted expression domain of *Fgf8* in the ectoderm of the hindlimb bud. The expression domain of *Gre* in the mesenchyme is also shifted to the anterior side in the early stage of limb development. In addition, the expression domains of *Gli1*, *ptc* and *dHAND*, which are restricted to the posterior side of wild-type limb buds, are expanded anteriorly. At later embryonic stages, ectopic *Shh* expression was observed at the anterior margin of the limb bud. Our results indicate that induction of ectopic *Shh* is not the primary defect of the *lx* mutation, but rather that the *lx* mutation affects the positioning of anteroposterior border in developing hindlimb buds. These results suggest that the *lx* gene functions to regulate the initial anteroposterior polarization of hindlimb buds, perhaps through defining the boundary of *Fgf8* expression domain in the surface ectoderm.

Results

Skeletal Phenotype of *lx*

The skeletal phenotype of *lx* mutants has been described in detail (Carter, 1951; Carter, 1953; Carter, 1954). The phenotype, however, is known to vary depending on the genetic background (Masuya *et al.*, 1997). We therefore established a *lx* homozygous line on the genetic background of the C57BL/6J strain by intercrossing of C57BL/6J-*lx*^{+/+}-*Kit*^{W^v} mice (see materials and methods). Since all progeny generated from the line showed hemimelia with shortened or missing tibia on their hindlimbs, the line was confirmed as homozygous for the *lx* mutation. Most of the *lx* homozygotes exhibited tibial hemimelia only on the right hindlimb (Fig. 1 A,B), with only a few mice displaying it bilaterally. They also showed hyperphalangy or anterior duplication of the first digit, either unilaterally or bilaterally in the hindlimbs (Fig. 1B). In addition to the limb defects, transformation of the 26th vertebra (hindmost lumber; L6) into the first sacral form was reproducibly observed. This posterior transformation caused the anterior shift in leg position (Fig. 1 C,D).

Heterozygous *lx* mice never showed the tibial hemimelia or the vertebral defects. They, however, did have an extra digit in the preaxial side of the hindlimbs (data not shown). No forelimb abnormalities were observed in either *lx* homozygotes or heterozygotes.

Shh-Fgf4 Feedback Loop in *lx* Mutant Mice

In many preaxial polydactylous mouse mutants including *lx*, ectopic expression of *Shh* and *Fgf4* is often observed at the anterior margin of developing limb buds (Masuya *et al.*, 1995; Masuya *et al.*, 1997). To clarify the precise patterns of *Shh* and *Fgf4* expression during *lx* limb development, we performed *in situ* hybridization using *lx* homozygous embryos. In wild-type hindlimb buds, *Shh* expression is first detected at the posterior margin of the mesenchyme at E10.5 (Fig. 2A), and is more strengthened in the developing ZPA at E11.5 (Fig. 2C). It becomes undetectable by E12.5. In *lx* hindlimb buds, *Shh* expression was first detected at E10.5 (Fig. 2B). Compared with wild-type mice, however, expression was notably more anterior in location. At E11.5, *lx* formed the narrow limb buds. At this stage, *Shh* was detected in the ZPA, but its expression domain was extended anteriorly (Fig. 2D). In addition, at this stage, a small focus of *Shh* expression was observed in the anterior margin of the hindlimb bud (arrowheads in Fig. 2 D,E). At E12.5, *Shh* was nearly undetectable in the posterior side of the *lx* hindlimb buds, whereas strong ectopic expression of *Shh* was detected in the anterior mesenchyme with ectopic outgrowth of the anterior tissue (data not shown). Activation of ectopic *Shh* in *lx* mutants showed a one-day lag compared with endogenous *Shh*.

Expression of *Fgf4* is induced by *Shh*, and *Fgf4*, in turn, maintains *Shh* expression during normal limb development (Lauer

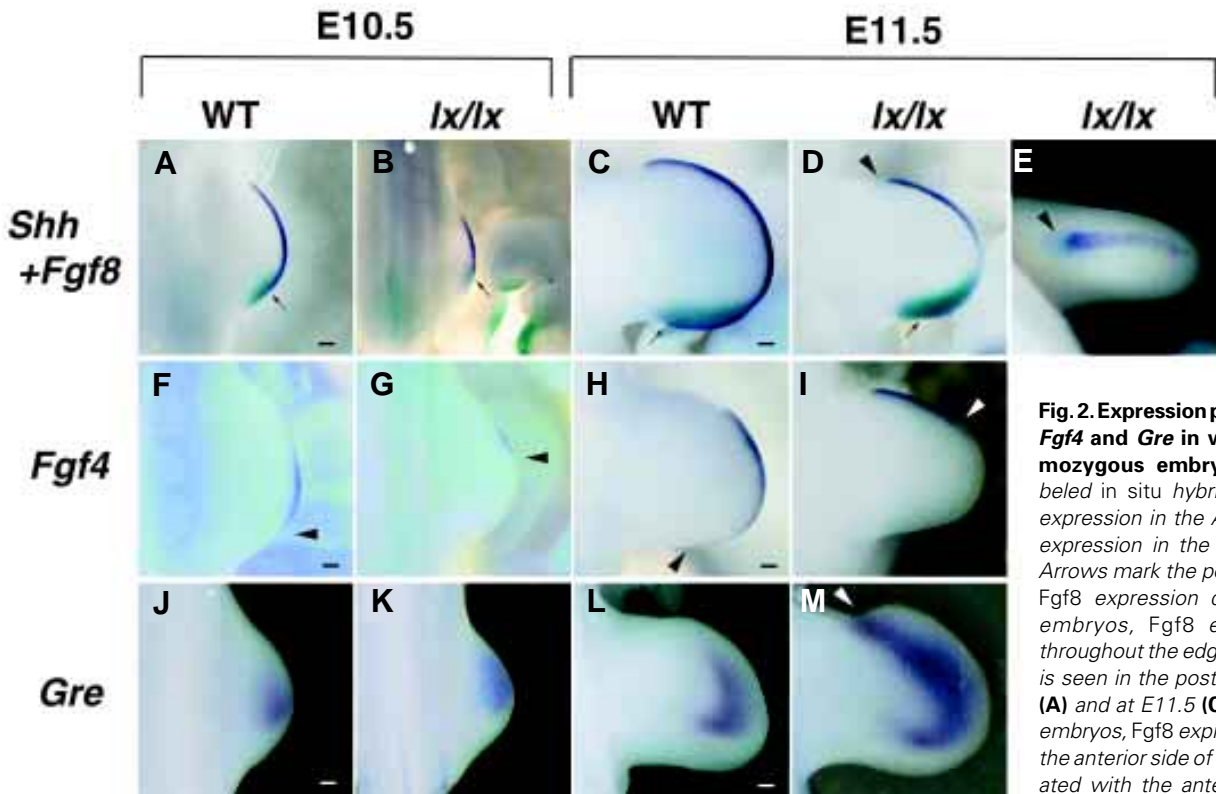


Fig. 2. Expression patterns of *Shh*, *Fgf8*, *Fgf4* and *Gre* in wild-type and *lx* homozygous embryos. (A-E) Double-labeled *in situ* hybridization shows *Fgf8* expression in the AER (purple) and *Shh* expression in the mesenchyme (blue). Arrows mark the posterior margin of the *Fgf8* expression domain. In wild-type embryos, *Fgf8* expression extends throughout the edge of the limb, and *Shh* is seen in the posterior margin at E10.5 (A) and at E11.5 (C). In *lx* homozygotes embryos, *Fgf8* expression is restricted to the anterior side of the ectoderm, associated with the anteriorized *Shh* expression at its margin at E10.5 (B). At E11.5

(D), *Fgf8* expression extends throughout the edge of the limb in *lx/lx*. Ectopic *Shh* is expressed in the anterior mesenchyme (arrowhead in D). (E) Anterior view of the *Shh* and *Fgf8* expression domain in *lx/lx*. *Shh* is expressed in the mesenchyme underlying the anterior end of the *Fgf8* expression domain. (F-I) Expression of *Fgf4* at E10.5 (F,G) and E11.5 (H,I). In *lx/lx*, *Fgf4* is shifted anteriorly (G, I) compared with wild type (F, H). Arrowheads indicate the posterior end of the *Fgf4* expression domain. (J-M) Expression of *Gre* in wild-type (J,L) and *lx/lx* (K,M) embryos. At E10.5 (J,K), *Gre* expression underlies *Fgf4* expression in the ectoderm of wild-type embryos. In E11.5 *lx* embryos (M), *Gre* expression is expanded to the anterior margin of the limb bud (arrowhead in M), overlapping with the ectopic *Shh* expression. Scale bar, 0.1 mm.

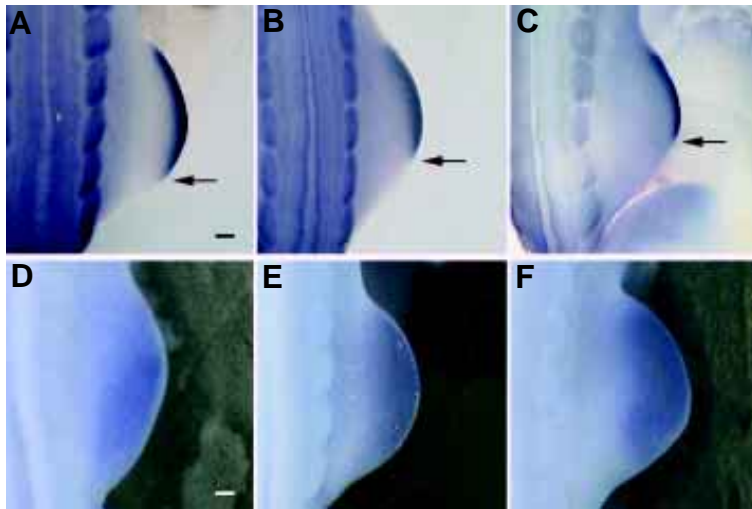


Fig. 3. Expression of *Fgf8* (A,B,C) in surface ectoderm and *Fgf10* (D,E,F) in mesenchyme in E10.5 wild-type (A,D), *lx/+* (B,E) and *lx/lx* (C,F) embryos. The arrows indicate the posterior margin of the *Fgf8* expression domain. The extent of *Fgf8* expression depends on the dose of the *lx* mutant gene (A-C), while the *Fgf10* expression domains are not affected (D-F). Scale bar, 0.1 mm.

et al., 1994; Niswander et al., 1994). In E10.5 wild-type embryos, *Fgf4* expression is initiated in the middle of the apical ectoderm (Fig. 2F). In the hindlimb of E10.5 *lx* embryos, *Fgf4* expression domain was shifted anteriorly in the apical ectoderm (Fig. 2G). In E11.5 wild-type embryos, *Fgf4* is detected in the posterior two-thirds of the AER, and the expression domain is directly overlays the *Shh* expression domain in the mesenchyme (Fig. 2H). In E11.5 *lx* embryos, *Fgf4* localized in the anterior AER, and was hardly detectable on the posterior side (Fig. 2I).

In normal limb development, Gremlin (*Gre*) is thought to maintain the positive feedback loop between *Shh* and *Fgf4*. In wild-type embryos, *Gre* is expressed in the posterior half of the mesenchyme in a region underlying *Fgf4* expression in the AER (Fig. 2J,L). In E10.5 *lx* hindlimb, the expression domains of both *Shh* and *Fgf4* were biased towards the anterior, and *Gre* was also expressed in the anterior half of the limb mesenchyme in parallel with the more anterior localization of *Fgf4* in the AER (Fig. 2G,K). In E11.5 *lx* hindlimb, *Gre* expression was activated in a wide range of the limb mesenchyme, where endogenous and ectopic *Shh* were expressed (Fig. 2M). This indicates that the signal between ectopic *Shh* and the AER is mediated through *Gre*, as is the case in normal development. Furthermore, in *lx* hindlimbs, *Shh*, *Fgf4* and *Gre* were shifted towards the anterior side of the limb bud in the initial stage of development.

Spatial Relationship of *Shh* and *Fgf8* Expression Domains

In normal limb development, the ZPA interacts with the AER to form the proper A-P and P-D axes. *Fgf8* is expressed throughout the whole AER, and the posterior end of the expression domain overlays the *Shh* expression domain in the ZPA (Fig. 2A,C). In E10.5 *lx* hindlimb buds, the *Fgf8* expression domain was reduced in size and was restricted to the anterior side of the apical ectoderm (Fig. 2B). The posterior end of the *Fgf8* expression domain overlaid the *Shh* expression domain. In E11.5 *lx* embryos, *Fgf8* was detected in the whole AER with the highest expression in the most

anterior end (Fig. 2D). Both ends of the *Fgf8* expression domain overlaid the *Shh* expression domain (Fig. 2D,E). In E11.5 *lx* hindlimbs, although *Fgf4* was not expressed in the posterior side (Fig. 2I), the *Fgf8* expression domain was overlapped with *Shh* in the posterior AER. Thus, *Fgf8*, but not *Fgf4*, likely functions to maintain the expression of *Shh* in *lx*.

Dose Dependent Effect of the *lx* Mutant Gene on *Fgf8* Expression

To control the initial outgrowth of hindlimbs, *Fgf10* in the mesenchyme induces *Fgf8* in the apical ectoderm. In the hindlimb buds of *lx* homozygotes, we detected anterior-restricted expression domain of *Fgf8*. To address the possibility of a dose-dependent effect of the *lx* mutant gene, expression of *Fgf8* was compared in *lx* heterozygotes, *lx* homozygotes, and wild-type embryos. The embryos studied were littermates derived from intercrossing *lx* heterozygotes. In wild-type hindlimbs, *Fgf8* expression in the apical ectoderm extended approximately 3 somites in width (Fig. 3A). In *lx* heterozygotes and homozygotes, *Fgf8* expression extended about 2.5 (Fig. 3B) and 2 somites in width (Fig. 3C), respectively. These data indicate that the *Fgf8* expression domain in the apical ectoderm of the hindlimb depends on the expression of the *lx* mutant gene in a dose-dependent manner. On the other hand, *Fgf10* was expressed similarly in whole limb mesoderm in the embryos regardless of *lx* genotype (Fig. 3D,E,F).

Excess Cell Death in *lx* Hindlimb Buds

Although *lx* mutants had normal hindlimb bud size at E10.5, at later stages, the hindlimb bud narrowed. In E10.5 *lx* hindlimbs, *Fgf8* was not expressed in the posterior side of the apical ectoderm raising the possibility that *lx* hindlimbs are defective in AER formation. Using E10.75 embryos, we performed Nile blue staining to detect cell death in the hindlimb buds. In wild type, no prominent cell death was observed in the AER (Fig. 4A). By contrast, *lx* mutants showed evidence of excess cell death in the posterior side of the apical ectoderm (Fig. 4B). The regression of the AER on the posterior side may cause hypoplasia of the hindlimb buds in *lx*.

A-P Axis Formation in *lx* Hindlimb Mesenchyme

Since the A-P axis was altered in *lx* hindlimb ectoderm, we examined axial formation in early stage limb mesenchyme. In E10.5 wild-type embryos, *Gli1* and the SHH receptor *Ptc* are expressed in the posterior side of the limb mesenchyme (Fig. 5

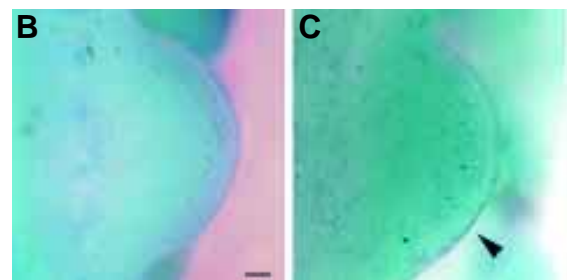


Fig. 4. Nile blue staining of E10.75 wild-type (A) and *lx/lx* hindlimb buds (B). Excess cell death is observed in the posterior side of the apical ectoderm in *lx* homozygotes (arrowhead in B). Scale bar, 0.1 mm.

A,C), and their expression domains overlaps with *Fgf4* expression. In E10.5 *lx* hindlimb buds, *Ptc* and *Gli1* expression was expanded to the whole mesenchyme (Fig. 5 B,D). In wild-type embryos, *Gli3* and *Alx4* are expressed at the anterior side of the limb mesenchyme (Fig. 5 E,G). In E10.5 *lx* hindlimb buds, the *Gli3* and *Alx4* expression domains in the anterior mesenchyme were slightly narrower than in wild type (Fig. 5 F,H). Our data indicate that the extent of the anterior mesenchyme was reduced in *lx* hindlimb buds from an early stage of the development. To confirm a reduction of the anterior mesenchyme in *lx*, we examined the expression of *dHAND*, which acts upstream of *Shh* and is expressed in the posterior mesenchyme of limb buds (Charité *et al.*, 2000). At E10.5, the *dHAND* expression domain was expanded in *lx* hindlimb buds compared with wild type (Fig. 6 A,B).

These results suggest that *lx* limb mesenchyme is composed from the narrowed anterior region and the expanded posterior region from the beginning of limb development. To elucidate the effects of *Alx4* and *Gli3* on *dHAND* expression, we examined the expression of *dHAND* in *Ist* and *Xt^J*, which are loss-of-function mutants of *Alx4* and *Gli3*, respectively (Hui and Joyner, 1993; Qu *et al.*, 1998). In E10.5 *Ist* limb buds, *dHAND* expression in the mesenchyme was normal (Fig. 6C). In *Xt^J* embryos, however, *dHAND* expression was expanded to the anterior region of the limb mesenchyme (Fig. 6D).

Discussion

Primary Defects of the *lx* Mutation

In E10.5 *lx* homozygote embryos, we observed anterior-restricted expression domain of *Fgf8* in the ectoderm of the hindlimb, as well as anteriorised expression domain of *Shh* (Fig. 2B). These were the earliest abnormalities recognized in *lx* homozygous embryos. Altered expression patterns of *Fgf8* and *Shh*, both of which are known to play key roles in outgrowth and patterning of limb buds, likely causes hemimelia and preaxial polydactyly of *lx* mutants displayed at later stages. We also observed that *lx* homozygotes reproducibly exhibited posterior transformation of the 6th lumbar vertebra into a sacral form (Fig. 1). Previous reports have shown that the *lx* mutation alters hindlimb positioning, leading to an anterior shift equivalent to the distance of 0.5-1 somite (Carter, 1954). Thus, the *lx* mutation appears to cause anterior positioning of the initial hindlimb field. A similar anterior shift of hindlimb position was observed in mouse mutants with disrupted expression of *Hoxd-11* and *Hoxd-10* in the trunk mesoderm (Gerard *et al.*, 1996), and in *gdf11* knockout mice (McPherron *et al.*, 1999). Notably, these other mutants did not show digital abnormality along the A-P axis, indicating that an anterior shift of limb position is not always associated with abnormalities in A-P axis formation within limb buds. Thus, the *lx* mutation is associated with two distinct defects in limb development. Firstly, the expression domains of *Fgf8* and *Shh* are altered in *lx* mutants. Secondly, the *lx* mutation affects positioning of the initial hindlimb field along the body axis.

In normal limb development, *Fgf10* expression in the lateral plate mesoderm induces *Fgf8* expression in the apical ectoderm of limb buds (Ohuchi *et al.*, 1997). *Fgf8* is the only gene among *Fgf* family members which is expressed before the induction of *Shh* (Crossley *et al.*, 1996). *Shh* knockouts show no alteration of *Fgf8* expression pattern (Sun *et al.*, 2000). Conversely, a conditional mutant lacking *Fgf8* in the AER shows delayed *Shh* expression (Lewandoski *et al.*,

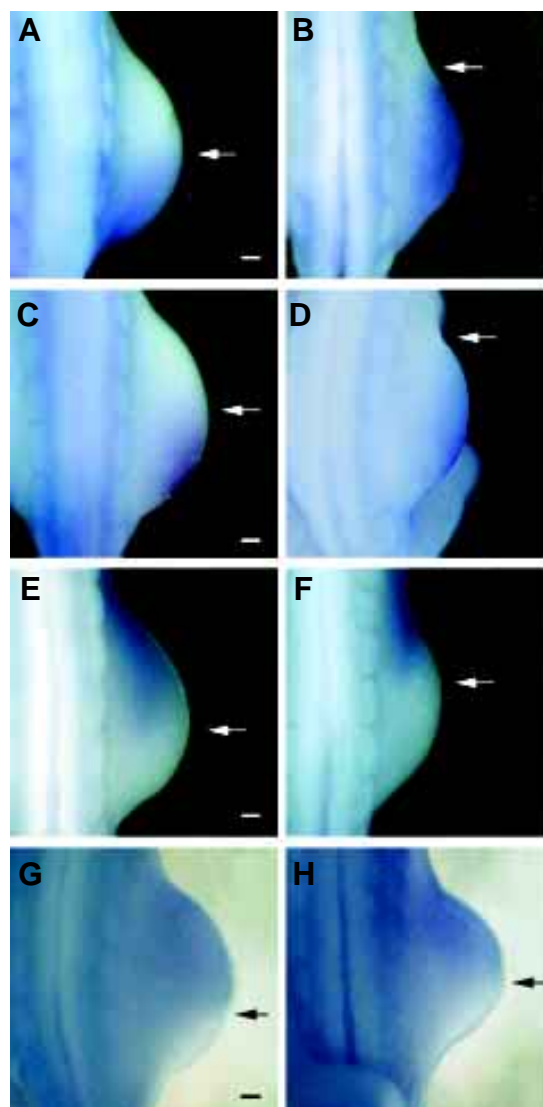


Fig. 5. Expression patterns of *Gli1* (A,B), *Ptc* (C,D), *Alx4* (E,F) and *Gli3* (G,H) in E10.5 wild-type (A,C,E,G) and *lx/lx* (B,D,F,H) hindlimb buds. Arrows indicate the anterior limits of *Gli1* and *Ptc* or the posterior limits of *Alx4* and *Gli3* in the limb mesenchyme. In *lx/lx*, *Gli1* (B) and *Ptc* (D) expression domains are extended to the anterior side, while the expression domains of *Alx4* (F) and *Gli3* (H) reduced in size. Scale bar, 0.1 mm.

2000). These reports suggest that *Fgf8* normally acts to induce *Shh* expression. Consideration of past results and the findings in this study raise the possibility that the defect underlying the phenotype in the *lx* mutant is due to altered regulation of *Fgf8* expression in the apical ectoderm of the limb bud. Since we observed no alteration in *Fgf10* expression in the mesoderm of the *lx* hindlimb buds, the primary defect caused by the *lx* mutation is likely to be in the regulation of *Fgf8* expression, possibly in receiving the *Fgf10* signal. In normal development, *Fgf8* in the intermediate mesoderm determines presumptive limb territory, and induces *Fgf10* in the lateral plate mesoderm. Thus, the anterior shift of the initial limb field in *lx* mutants might be due to a defect in *Fgf8* expression in the intermediate mesoderm in the earlier developmental stage.

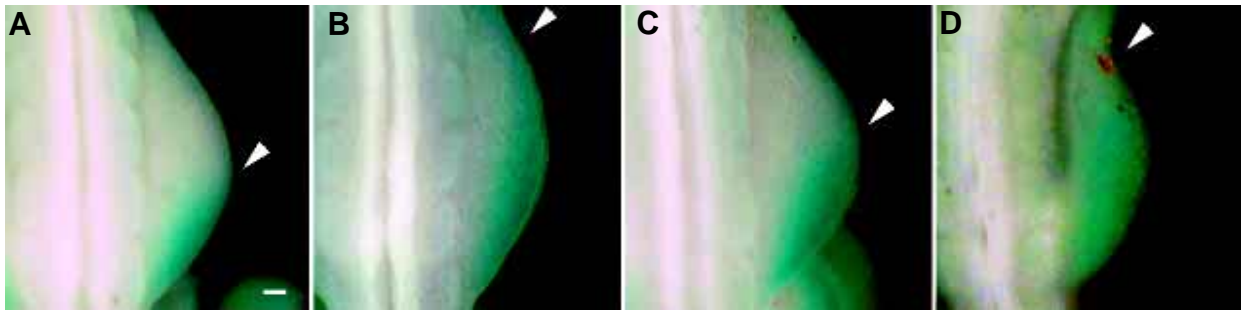


Fig. 6. Expression of *dHAND* in hindlimb buds of E10.5 wild type (A), *lx* homozygote (B), *lst* homozygote (C) and *Xt* homozygote (D). Arrowheads indicate the anterior margin of the *dHAND* expression domain in the limb bud. The *dHAND* expression domain is expanded in *lx*/*lx* and *Xt*/*Xt*, but unaffected in *lst*/*lst*. Scale bar, 0.1 mm.

Induction of *Shh* and Margins of the *Fgf8* Expression Domain

By simultaneous detection of the expression of *Shh* and *Fgf8* in this study, we observed that *Shh* was induced in the mesenchyme underlying the posterior end of the *Fgf8* expression domain in wild-type limb buds (Fig. 2A). A similar spatial relationship between the posterior end of *Fgf8* expression domain and the position of *Shh* induction was also observed in *lx* mutants, despite the more anterior localization of both molecules was observed (Fig. 2B). Likewise, we also observed that in E11.5 *lx* hindlimb buds, ectopic *Shh* expression was induced in the mesenchyme under the anterior end of the *Fgf8* expression domain (Fig. 2D). Thus, both margins of *Fgf8* expression domain appear to have the potential to induce *Shh* expression, although additional factors may also be involved.

Control of Limb Bud Size by *Fgf8*

In this study, we found that the size of the hindlimb bud is normal in *lx* homozygous and heterozygous embryos when they first emerge from the trunk, suggesting that the initial hindlimb territory of *lx* mutants contains the same mass of mesenchyme as wild-type mice. In fact, *Fgf10* is expressed throughout the whole limb mesenchyme in *lx* limb buds. In later stages, *lx* mutants developed narrowed hindlimb buds due to excess cell death, which is probably

caused by the absence of *Fgf8* expression in the posterior apical ectoderm (Fig. 4). Therefore, while the expression of *Fgf8* in surface ectoderm is not essential for the initiation of hindlimb outgrowth and determination of hindlimb size, it is required to promote cell proliferation. This is also supported by the previous studies of mice lacking *Fgf8* expression in limb ectoderm. These mutants develop normally sized limbs in the early stage, which then become narrow in later stages (Lewandoski et al., 2000).

Function of *dHAND* and *Gli3* in A-P Border Formation in Limb Mesenchyme

The A-P axis in *lx* hindlimb bud was shifted to the anterior side in both the ectoderm and the mesenchyme prior to ectopic *Shh* expression. Transgenic mice overexpressing *dHAND* throughout the hindlimb bud show ectopic induction of *Shh* (Charité et al., 2000), suggesting that *dHAND* functions to induce *Shh* in normal limb development. On the other hand, *Gli3* and *Alx4* are negative regulators of *Shh* (Masuya et al., 1995; Qu et al., 1997; Qu et al., 1998). Ectopic expression of *dHAND* results in repression of *Gli3* expression in chick limbs (Fernandez-Teran et al., 2000). In this study, we found expansion of *dHAND* expression domain in *lx* mutants, accompanied with a reduction of the size of *Gli3* and the *Alx4* expression domains (Fig. 6B). In addition, the *Xt* mutant displayed *dHAND* expression throughout the limb bud in the absence of *Gli3* (Fig. 6D). *Gli3* and *Alx4* have been reported to act in parallel pathways in limb formation (Takahashi et al., 1998). Therefore, in normal limb development, *Gli3* and *dHAND* likely down-regulate one another reciprocally, which may contribute to determination of the A-P border in limb mesenchyme and to the formation of the proper A-P axis.

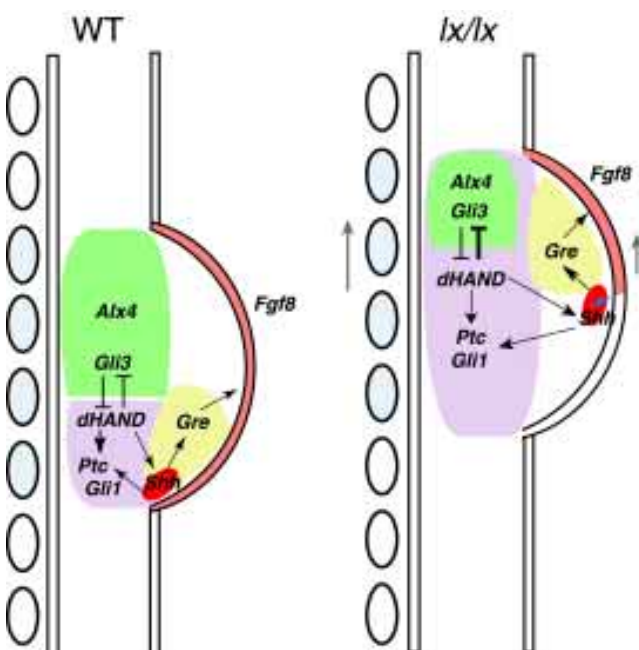


Fig. 7. Summary of expression patterns of several key genes in limb development of *lx* embryos. (Left) In the wild-type limb mesenchyme, *Alx4* and *Gli3* are expressed in the anterior side. *Shh* expressed in the ZPA activates downstream genes such as *Ptc*, *Gli1* and *Gre*. *Gre* mediates the signal between the ZPA and the AER. The expression domains of *dHAND* and *Gli3* are controlled by reciprocal downregulation. (Right) *lx* homozygotes have normal hindlimb bud size during early stages of development, but their position is shifted to the anterior side along the body axis. The A-P axis of the limb bud is altered both in the mesenchyme and the ectoderm. *Shh* is induced in the mesenchyme underlying the anteriorly shifted end of the *Fgf8* expression domain (blue arrow). *dHAND* expression is expanded throughout the hindlimb bud. The *lx* gene likely plays at least two distinct roles in positioning of the hindlimb bud along the body axis and regulation of *Fgf8* expression in the surface ectoderm (indicated by gray arrows).

In addition to a role as an upstream activator of *Shh*, ectopic expression of *dHAND* induces expression of *Shh* downstream genes, such as *Gli1* and *Ptc*, without activation of *Shh* in the chick limbs (Fernandez-Teran *et al.*, 2000). In *lx* mutants, *Gli1* and *Ptc* were activated throughout the limb mesenchyme prior to the ectopic activation of *Shh*, and their expression domains were overlapped with the *dHAND* expression domain (Fig. 5). Thus, our data suggest that *dHAND* has the potential to activate the *Shh* downstream genes *Gli1* and *Ptc*, independent of *Shh*. On the other hand, *Gre* expression was reported to be normal in the absence of *dHAND* (Charité *et al.*, 2000). The present study indicates that *Gre* is not expressed in the posterior side of *lx* hindlimb bud (Fig. 2L). *Gre* expression, therefore, is not influenced by *dHAND*. All available data suggest the presence of at least two signaling pathways for the induction of *Shh* downstream genes, *dHAND*-dependent and -independent ones.

Polydactyly in *lx* Homozygotes

In preaxial polydactyly mouse mutants, ectopic expression of *Shh* is often observed in the anterior margin of their limb buds. The mutated genes have been proposed to repress *Shh* expression in the anterior mesenchyme of limb buds (Masuya *et al.*, 1997). In the case of the *lx* mutation, the earliest ectopic expression of *Shh* was detected at E11.5. At this stage the reduced limb size, phenotype characteristic of *lx*, had already been apparent. Thus, ectopic *Shh* is unlikely to be the primary defect. Within the *lx* hindlimb bud, the A-P border was shifted to the anterior side from the initial stage of limb development, as summarized in Fig. 7. As a result, genes that determine the posterior identity of the limb had expanded in the *lx* hindlimb bud. Among them, *dHAND* induces *Shh* in normal limb development, and its overexpression causes ectopic *Shh* expression, leading to preaxial polydactyly and tibial hemimelia (Charité *et al.*, 2000). Thus, expanded expression of *dHAND* in the anterior mesenchyme might induce ectopic *Shh* expression, leading to the altered skeletal patterning of *lx* hindlimbs.

In the mouse polydactylous mutant Dominant hemimelia (*Dh*), *Fgf8* domain is shifted anteriorly in the apical ectoderm and activation of ectopic *Shh* occurs at E12.5 (Lettice *et al.*, 1999). The gene expression patterns shown in *Dh* heterozygotes resemble those of *lx* homozygotes. *Dh* heterozygotes show tibial hemimelia and reduction of the lumbar vertebrae (Searle, 1964), which is similar to the skeletal phenotype of *lx* homozygotes. Furthermore, *Dh* hindlimb buds are narrower than those of wild-type mice and the limb position is shifted to the anterior by 2-3 somites. Thus, *Dh* and *lx* may be located in the same signaling pathway to establish the A-P axis of hindlimb. In this context, we await the examination of whether *Dh* shows anterior expansion of *dHAND* expression.

Materials and Methods

lx mice

C57BL/6J-*lx*⁺-*Kit*^{W^v} mice were purchased from The Jackson Laboratory (Bar Harbor, Me., USA), and maintained by backcrossing to C57BL/6J (B6) in the Genetic Strain Resource Center, National Institute of Genetics (NIG) (Mishima, Japan). To generate a homozygous *lx* line, we obtained progeny from the intercross of B6-*lx*⁺-*Kit*^{W^v} mice and selected for progeny showing hemimelia. After 10 generations of repeating sib-mating, the homozygous line was established. All progeny generated from the line show hemimelia. For whole-mount *in situ* hybridization, embryos were obtained from intercrossing of the homozygotes.

Consonic Strain and Generation of *lx* Heterozygotes

A consomic strain, B6.MSM-Chr5, was established at NIG. In this strain, Chromosome 5 derived from the MSM strain (Japanese wild-mouse origin) was introduced into the genetic background of B6. The chromosome was maintained in the heterozygous state by backcrossing to B6. Mice heterozygous for the *lx* mutation were obtained from crosses of the *lx* homozygous line and B6.Chr5-MSM. In the resultant progeny, the genotype of the region flanking the *lx* locus was determined based on polymorphisms of microsatellite markers. For *in situ* hybridization, embryos were obtained from intercrosses of the heterozygotes. The genotype of the *lx*-linked region in the progeny was determined using genomic DNA, which was PCR-amplified with the primers, *D5Mit146*, *D5Mit5*, *D5Mit9*, and *D5Mit287*. The genomic DNA was isolated from adult ears or fetal yolk sacs using a protocol modified from Laird *et al.* (1991).

Ist Mice

B6C3-*a/a-Ist*⁺ mice were purchased from The Jackson Laboratory. For whole-mount *in situ* hybridization, embryos were obtained by intercrossing heterozygotes. Genomic DNA was isolated from fetal yolk sacs. Embryos were genotyped by PCR-amplification with primers flanking the mutated region of *Alx4* gene (primers: 5'-GCTGGAGAAAGTCTTCCAGAAG-3' and 5'-AGTTGGGTTAAATTGCGTA TGG-3') (Qu *et al.*, 1998).

Xt Mice

C3HeB/FeJ-Eso/Eso-*Xt*⁻ mice were purchased from The Jackson Laboratory. For whole-mount *in situ* hybridization, embryos were obtained by intercrossing heterozygotes. Homozygotes were identified according to morphological features (Franz, 1994).

Skeletal Preparations

Double staining of the skeleton with alcian blue and alizarine red was performed essentially as described elsewhere (Wallin *et al.*, 1994).

Whole-Mount *In Situ* Hybridization

Single-labeled whole-mount *in situ* hybridization using digoxigenin-UTP (Roche) labeled RNA probes was carried out as described by Wilkinson *et al.* (1992). For signal detection, a color reaction using NBT and/or BCIP (Roche) was performed. Simultaneous detection of two transcripts using double-color *in situ* hybridization was carried out as described by Hecksher-Sørensen *et al.* (1998). Digoxigenin-UTP and fluorescein-UTP (Roche) labeled RNA probes were hybridized at the same time and detected using BCIP and NBT. The *dHAND* probe was generated from the entire murine *dHAND* coding region (Srivastava *et al.*, 1995). The *Alx4* probe is a 648bp fragment including the paired tail domain (nucleotides 1077-1724). Photographs were taken using Keyence (Osaka, Japan) VH-8000 system.

Nile Blue Sulphate Staining of Dead Cells

Dead cells were stained with Nile blue sulphate (MERCK) as described by A. S. W. Shum *et al.* (1999). Embryos were explanted into PBS, bathed in Nile blue sulphate dissolved in lactated Ringer's solution (1 / 50,000) for 15 min at 37°C, and then washed in Ringer's solution.

Acknowledgements

We are grateful to Dr. A. McMahon for the *Shh* probe, Dr. G. Martin for the *Fgf4* probe, Dr. T. Sakurai for the *Fgf8* probe, Dr. B. Hogan for the *Fgf10* probe, Dr. A. Kuroiwa for the *Gre* probe, Dr. A. Joyner for the *Gli1* probe, Dr. C. C. Hui for the *Gli3* probe and Dr. M. Scott for the *Ptc* probe. We also thank K. Abe, K. Aida and M. Arai for maintenance of mice. This study was supported in part by grants in aid from the Ministry of Education, Culture, Sports, Science and Technology of Japan. This paper is contribution no. 2466 from the National Institute of Genetics, Japan.

References

- CAPDEVILA, J., TSUKUI, T., RODRIGUEZ-ESTEBAN, C., ZAPPAVIGNA, V. and IZPISÚA-BELMONTE, J.C. (1999). Control of vertebrate limb outgrowth by the proximal factor *Meis2* and distal antagonism of BMPs by Gremlin. *Mol. Cell* 4: 839-849.
- CARTER, T.C. (1951). The genetics of luxate mice. I. Morphological abnormalities of heterozygotes and homozygotes. *J. Genet.* 50: 441-457.
- CARTER, T.C. (1953). The genetics of luxate mice. III. Horseshoe kidney, hydronephrosis and lumbar reduction. *J. Genet.* 51: 441-457.
- CARTER, T.C. (1954). The genetics of luxate mice. IV. Embryology. *J. Genet.* 52: 1-35.
- CHARITÉ, J., MCFADDEN, D.G. and OLSON, E.N. (2000). The bHLH transcription factor dHAND controls *Sonic hedgehog* expression and establishment of the zone of polarizing activity during limb development. *Development* 127: 2461-2670.
- COLVIN, J.S., FELDMAN, B., NADEAU, J.H., GOLDFARB, M. and ORNITZ, D.M. (1999). Genomic organization and embryonic expression of the mouse *fibroblast growth factor 9* gene. *Dev. Dyn.* 216: 72-88.
- CROSSLEY, P.H., MINOWADA, G., MACARTHUR, C.A. and MARTIN, G.R. (1996). Roles for FGF8 in the induction, initiation, and maintenance of chick limb development. *Cell* 84: 127-136.
- FERNANDEZ-TERAN, M., PIEDRA, M.E., KATHIRIYA, I.S., SRIVASTAVA, D., RODRIGUEZ-REY, J.C. and ROS, M.A. (2000). Role of dHAND in the anterior-posterior polarization of the limb bud: implications for the *Sonic hedgehog* pathway. *Development* 127: 2133-2142.
- FRANZ, T. (1994). Extra-toes (*Xt*) homozygous mutant mice demonstrate a role for the *Gli-3* gene in the development of the forebrain. *Acta. Anat.* 150: 38-44.
- GERARD, M., CHEN, J.Y., GRONEMEYER, H., CHAMBON, P., DUBOULE, D. and ZAKANY, J. (1996). In vivo targeted mutagenesis of a regulatory element required for positioning the *Hoxd-11* and *Hoxd-10* expression boundaries. *Genes Dev.* 10: 2326-2334.
- HECKSHER-SØRENSEN, J., HILL, R.E. and LETTICE, L. (1998). Double labeling for whole-mount *in situ* hybridization in mouse. *Biotechniques* 24: 914-918.
- HSU, D.R., ECONOMIDES, A.N., WANG, X., EIMON, P.M. and HARLAND, R.M. (1998). The *Xenopus* dorsalizing factor Gremlin identifies a novel family of secreted proteins that antagonize BMP activities. *Mol. Cell* 1: 673-683.
- HUI, C.-C. and JOYNER, A.L. (1993). A mouse model of Greig cephalopolysyndactyly syndrome: the extra-toes' mutation contains an intragenic deletion of the *Gli3* gene. *Nat. Genet.* 3: 241-245.
- LAIRD, P.W., ZIJDERVELD, A., LINDERS, K., RUDNICKI, M.A., JAENISCH, R. and BERNS, A. (1991). Simplified mammalian DNA isolation procedure. *Nucleic Acids Res.* 19: 4293.
- LANE, P.W. (1967). Linkage groups III and XVII in the mouse and the position of the light-ear locus. *J. Hered.* 58: 21-24.
- LAUFER, E., NELSON, C.E., JOHNSON, R.L., MORGAN, B.A. and TABIN, C. (1994). *Sonic hedgehog* and *Fgf-4* act through a signalling cascade and feedback loop to integrate growth and patterning of the developing limb bud. *Cell* 79: 993-1003.
- LETTICE, L., HECKSHER-SØRENSEN, J. and HILL, R.E. (1999). The dominant hemimelia mutation uncouples epithelial-mesenchymal interactions and disrupts anterior mesenchyme formation in mouse hindlimbs. *Development* 126: 4729-4736.
- LEWANDOSKI, M., SUN, X. and MARTIN, G.R. (2000). *Fgf8* signaling from the AER is essential for normal limb development. *Nat. Genet.* 26: 460-463.
- MASUYA, H., SAGAI, T., WAKANA, S., MORIWAKI, K. and SHIROISHI, T. (1995). A duplicated zone of polarizing activity (ZPA) in polydactylous mouse mutants. *Genes Dev.* 9: 1645-1653.
- MASUYA, H., SAGAI, T., MORIWAKI, K. and SHIROISHI, T. (1997). Multigenic control of the localization of the zone of polarizing activity in limb morphogenesis in the mouse. *Dev. Biol.* 182: 42-51.
- MCPHERRON, A.C., LAWLER, A.M. and LEE, S.J. (1999). Regulation of anterior/posterior patterning of the axial skeleton by *growth/differentiation factor 11*. *Nat. Genet.* 22: 260-264.
- MERINO, R., RODRIGUEZ-LEON, J., MACIAS, D., GAÑAN, Y., ECONOMIDES, A.N. and HURLE, J.M. (1999). The BMP antagonist Gremlin regulates outgrowth, chondrogenesis and programmed cell death in the developing limb. *Development* 126: 5515-5522.
- MOON, A.M., BOULET, A.M. and CAPECCHI, M.R. (2000). Normal limb development in conditional mutants of *Fgf4*. *Development* 127: 989-996.
- NISWANDER, L., TICKLE, C., VOGEL, A., BOOTH, I. and MARTIN, G.R. (1993). FGF-4 replaces the apical ectodermal ridge and directs outgrowth and patterning of the limb. *Cell* 75: 579-587.
- NISWANDER, N., JEFFREY, S., MARTIN, G.R. and TICKLE, C. (1994). A positive feedback loop coordinates growth and patterning in the vertebrate limb. *Nature* 371: 609-612.
- OHUCHI, H., NAKAGAWA, T., YAMAMOTO, A., ARAGA, A., OHATA, T., ISHIMARU, Y., YOSHIOKA, H., KUWANA, T., NOHNO, T., YAMASAKI, M., ITOH, N. and NOJI, S. (1997). The mesenchymal factor, FGF10, initiates and maintains the outgrowth of the chick limb bud through interaction with FGF8, an apical ectodermal factor. *Development* 124: 2235-2244.
- QU, S., NISWANDER, K.D., JI, Q., VAN DER MEER, R., KEENEY, D., MAGNUSON, M.A. and WISDOM, R. (1997). Polydactyly and ectopic ZPA formation in *Alx-4* mutant mice. *Development* 124: 3999-4008.
- QU, S., TUCKER, S.C., EHRLICH, J.S., LEVORSE, J.M., FLAHERTY, L.A., WISDOM, R. and VOGT, T.F. (1998). Mutations in mouse *Aristaless-like4* cause Strong's luxoid polydactyly. *Development* 125: 2711-2721.
- RIDDLE, R.D., JOHNSON, R.L., LAUFER, E. and TABIN, C. (1993). *Sonic Hedgehog* mediates the polarizing activity of ZPA. *Cell* 75: 1401-1416.
- SAUNDERS, J.W.JR. (1948). The proximo-distal sequence of the origin of the parts of the chick wing and the role of the ectoderm. *J. Exp. Zool.* 108: 363-404.
- SAUNDERS, J.W. and GASSELING, M.T. (1968). Ectodermal-mesenchymal interactions in the origin of limb symmetry. In *Epithelial mesenchymal interactions*, (ed. R. Fleischmajer and R. E. Billingham), Williams and Wilkins, pp. 78-97.
- SEARLE, A.G. (1964). The genetics and morphology of two 'luxoid' mutants in the house mouse. *Genet. Res.* 5: 171-197.
- SHUM, A.S., POON, L.L., TANG, W.W., KOIDE, T., CHAN, B.W., LEUNG, Y.C., SHIROISHI, T. and COPP, A.J. (1999). Retinoic acid induces down-regulation of *Wnt-3a*, apoptosis and diversion of tail bud cells to a neural fate in the mouse embryo. *Mech. Dev.* 84: 17-30.
- SRIVASTAVA, D., CSERJESI, P. and OLSON, E.N. (1995). A subclass of bHLH proteins required for cardiac morphogenesis. *Science* 270: 1995-1999.
- SUN, X., LEWANDOSKI, M., MEYERS, E.N., LIU, Y.H., MAXSON, R.E., JR. and MARTIN, G.R. (2000). Conditional inactivation of *Fgf4* reveals complexity of signalling during limb bud development. *Nat. Genet.* 25: 83-86.
- TAKAHASHI, M., TAMURA, K., BUSCHER, D., MASUYA, H., YONEI-TAMURA, S., MATSUMOTO, K., NAITOH-MATSUO, M., TAKEUCHI, J., OGURA, K., SHIROISHI, T., OGURA, T. and IZPISÚA-BELMONTE, J.C. (1998). The role of *Alx-4* in the establishment of anteroposterior polarity during vertebrate limb development. *Development* 125: 4417-4425.
- TICKLE, C., SUMMERBELL, D. and WOLPERT, L. (1975). Positional signalling and specification of digits in chick limb morphogenesis. *Nature* 254: 199-202.
- TICKLE, C. (1981). The number of polarizing region cells required to specify additional digits in the developing chick wing. *Nature* 289: 295-298.
- WALLIN, J., WILTING, J., KOSEKI, H., FRITSCH, R., CHRIST, B. and BALLING, R. (1994). The role of *Pax-1* in axial skeleton development. *Development* 120: 1109-1121.
- WILKINSON, D.G. (1992). Whole mount *in situ* hybridization of vertebrate embryos. In *In Situ Hybridization: A Practical Approach*, (ed. Wilkenson, D. G.), University Press, Oxford, pp. 75-83.
- ZÚÑIGA, A., HARAMIS, A.P., MCMAHON, A.P. and ZELLER, R. (1999). Signal relay by BMP antagonism controls the SHH/FGF4 feedback loop in vertebrate limb buds. *Nature* 401: 598-602.